JACS
JOURNAL OF THE AMERICAN CHEMICAL SOCIETY
Article
pubs.acs.org/JACS

X-ray Crystallographic Characterization of New Soluble Endohedral Fullerenes Utilizing the Popular C_{82} Bucky Cage. Isolation and Structural Characterization of Sm@C_{3v}(7)-C_{82}, Sm@C_s(6)-C_{82}, and Sm@C_2(5)-C_{82}

Hua Yang,[†] Hongxiao Jin,[†] Xinqing Wang,[†] Ziyang Liu,*[,†,‡] Meilan Yu,[‡] Fukun Zhao,[‡] Brandon Q. Mercado,[§] Marilyn M. Olmstead,*[,§] and Alan L. Balch*[,§]

[†]College of Materials Science and Engineering, China Jiliang University, Hangzhou 310018, China
[‡]College of Life Science, Zhejiang Sci-Tech University, Hangzhou 310018, China
[§]Department of Chemistry, University of California, One Shields Avenue, Davis, California 95616, United States

Supporting Information

ABSTRACT: Three isomers of Sm@C_{82} that are soluble in organic solvents were obtained from the carbon soot produced by vaporization of hollow carbon rods doped with Sm_2O_3/graphite powder in an electric arc. These isomers were numbered as Sm@C_{82}(I), Sm@C_{82}(II), and Sm@C_{82}(III) in order of their elution times from HPLC chromatography on a Buckyprep column with toluene as the eluent. The identities of isomers, Sm@C_{82}(I) as Sm@C_s(6)-C_{82}, Sm@C_{82}(II) as Sm@C_{3v}(7)-C_{82}, and Sm@C_{82}(III) as Sm@C_2(5)-C_{82}, were determined by single-crystal X-ray diffraction on cocrystals formed with Ni(octaethylporphyrin). For endohedral fullerenes like La@C_{82}, which have three electrons transferred to the cage to produce the $M^{3+}@(C_{82})^{3-}$ electronic distribution, generally only two soluble isomers (*e.g.*, La@C_{2v}(9)-C_{82} (major) and La@C_s(6)-C_{82} (minor)) are observed. In contrast, with samarium, which generates the $M^{2+}@(C_{82})^{2-}$ electronic distribution, five soluble isomers of Sm@C_{82} have been detected, three in this study, the other two in two related prior studies. The structures of the four Sm@C_{82} isomers that are currently established are Sm@C_2(5)-C_{82}, Sm@C_s(6)-C_{82}, Sm@C_{3v}(7)-C_{82}, and Sm@C_{2v}(9)-C_{82}. All of these isomers obey the isolated pentagon rule (IPR) and are sequentially interconvertable through Stone–Wales transformations.

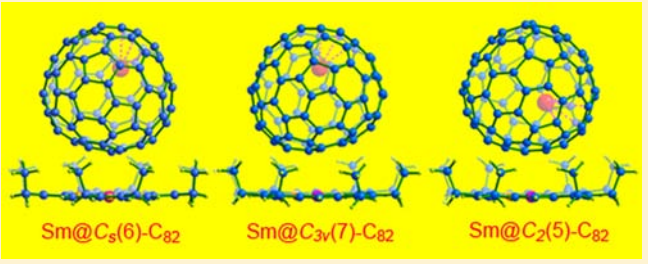

INTRODUCTION

The interior space of fullerenes offers the chemist an unusual environment in which a variety of atoms, molecules, and atomic clusters can be trapped to form an endohedral fullerene.[1,2] Despite their isolation, the trapped entities retain their physical properties such as light absorption and emission, magnetism, and nuclear stability. Consequently, these endohedrals have numerous potential applications in optoelectronic devices, solar energy collection, magnetic resonance imaging, and nuclear medicine.[3−5]

The simplest soluble endohedral fullerenes contain only a single atom. When that atom is an electropositive metal, electrons are transferred from the metal onto the empty π-type orbitals of the carbon cage so that an electronic structure of the type $M^{x+}@(C_{2n})^{x-}$ results.[6,7] For most lanthanide metals, including Sc, Y, La, Ce, Pr, Nd, Gd, Tb, Dy, Ho, Er, and Lu, three electrons are transferred to the cage to produce the $M^{3+}@(C_{2n})^{3-}$ type structure. The alkaline earth endohedrals adapt an $M^{2+}@(C_{2n})^{2-}$ type structure, which is also observed for the less electropositive lanthanides: Sm, Eu, Tm, and Yb.

Endohedral fullerenes that utilize the C_{82} cage are among the most intensively studied molecules of this type. Indeed, La@C_{82} was the first soluble endohedral to undergo purification and isolation.[8] Subsequently, numerous C_{82}-endohedrals enclosing one or two metal atoms or metal atom/main group atom clusters have been detected and isolated.[1,2] Considerable effort has been expended to produce covalently bonded adducts of the family of $M^{3+}@(C_{82})^{3-}$ endohedrals.[9] For the C_{82} cage, there are nine possible isomers that obey the isolated pentagon rule (IPR), which ensures cage stability by avoiding the steric stain caused when two pentagons abut.[10] The particular cage that is used for an individual endohedral depends upon the species entrapped and the number of electrons that are transferred to the cage.[6,7]

When six electrons are transferred to the cage, as is the case for $Gd_3N@C_s$(39663)-C_{82}, a non-IPR cage, a Bucky egg, with one pair of adjacent pentagons is utilized.[11] Consequently, it appears that none of the nine isomers that obey the IPR are

Received: May 18, 2012
Published: August 3, 2012

   dx.doi.org/10.1021/ja304867j | J. Am. Chem. Soc. 2012, 134, 14127−14136

suitable to house this trimetallic nitride cluster. However, for endohedral fullerenes of the type $Er_2@C_{82}$, IRP-obeying cages are used in the isomers Er2@C_s(6)-C82[12] and $Er_2@C_{3v}$(8)-C82.[13]

For endohedral fullerenes containing metal ions or clusters that can transfer four electrons to the cage, the preferred cage isomers are $[C_s(6)\text{-}C_{82}]^{4-}$ and $[C_{3v}(8)\text{-}C_{82}]^{4-}$. Computational studies suggest that the $[C_{3v}(8)\text{-}C_{82}]^{4-}$ should be the most stable at 0 K, but entropic factors cause the $[C_s(6)\text{-}C_{82}]^{4-}$ isomer to become more stable at higher temperatures.[14,15] Several endohedral fullerenes of this type have been characterized by single-crystal X-ray diffraction in pristine form, including $Sc_2(\mu_2\text{-}S)@C_s(6)\text{-}C_{82}$ and $Sc_2(\mu_2\text{-}S)@C_{3v}(8)\text{-}C_{82}$,[16] $Sc_2(\mu_2\text{-}C_2)@C_{3v}(8)\text{-}C_{82}$,[17] $Sc_2(\mu_2\text{-}O)@C_s(6)\text{-}C_{82}$,[18,19] along with $Sc_2(\mu_2\text{-}C_2)@C_s(6)\text{-}C_{82}$.[20]

For soluble molecules like $La@C_{82}$, which have three electrons transferred to the cage to produce the $M^{3+}@(C_{82})^{3-}$ electronic distribution, the most prevalent isomer utilizes another type of cage, the $C_{2v}(9)\text{-}C_{82}$ isomer.[21] $La@C_{2v}(9)\text{-}C_{82}$ has been characterized crystallographically both as exohedral adducts and in pristine form.[22−24] A minor soluble isomer of $La@C_{82}$, $La@C_s(6)\text{-}C_{82}$, has also been characterized through ^{13}C NMR spectroscopic measurements.[25]

When only two electrons are available for transfer as is the case for endohedrals containing Ca, Sm, Eu, Tm, and Yb, a more extensive series of soluble isomers of $M@C_{82}$ is formed. For example, four isomers of $Ca@C_{82}$ have been isolated.[26,27] Of these isomers, $Ca@C_{82}$(I) is the first to elute during high pressure liquid chromatography, $Ca@C_{82}$(II) is the second to elute, and so forth. ^{13}C NMR studies have identified the symmetry of these isomers as follows: $Ca@C_{82}$(I), one of three C_s isomers; $Ca@C_{82}$(II), one of two C_{3v} isomers; $Ca@C_{82}$(III), one of three C_2 isomers; and $Ca@C_{82}$(IV), the C_{2v} isomer.[28] Further insight into the structure of $M^{2+}@(C_{2n})^{2-}$ type endohedrals was obtained through a study of the ^{13}C NMR spectra of $Yb@C_{82}$ coupled with DFT computations that simulated the spectra.[29] That work identified three of the $Yb@C_{82}$ isomers as $Yb@C_s(6)\text{-}C_{82}$, $Yb@C_2(5)\text{-}C_{82}$, and $Yb@C_{2v}(9)\text{-}C_{82}$. However, no crystallographic work has been performed on any of the $M^{2+}@(C_{2n})^{2-}$ type endohedrals.

Here, we report the isolation of three isomers of a $M^{2+}@(C_{2n})^{2-}$ type endohedral, $Sm@C_{82}$, and their crystallographic characterization. Crystallographic data on endohedral fullerenes are particularly valuable, because they can provide information regarding which cage isomer is present, the positioning of the metals inside the cage, and the metric dimensions of the molecule. Such studies can be conducted on samples that would be too small to give ^{13}C NMR data, whose analysis would also be complicated by the presence of the paramagnetic samarium ion. Previous studies of $Sm@C_{82}$ endohedrals by Okazaki *et al.* reported the isolation of three isomers,[30,31] while Liu *et al.* reported the identification of four isomers of $Sm@C_{82}$.[32]

RESULTS

Isolation of Three Isomers of $Sm@C_{82}$. As described previously, carbon soot containing the samarium endohedral fullerenes was obtained by electric arc vaporization of hollow graphite rods filled with Sm_2O_3 and graphite powder.[33,34] The soot produced by this arc process was extracted with *o*-dichlorobenzene under sonocation. After concentration, the soluble extract was subjected to a four-stage, high-pressure liquid chromatographic (HPLC) process involving three complementary chromatographic columns (Buckyprep, Buckyprep-M, and 5PBB) with either chlorobenzene or toluene as the eluent. Three isomers of $Sm@C_{82}$ were identified and purified. Figure 1 shows the HPLC chromatograms of the purified samples of the $Sm@C_{82}$ isomers on a Buckyprep column.

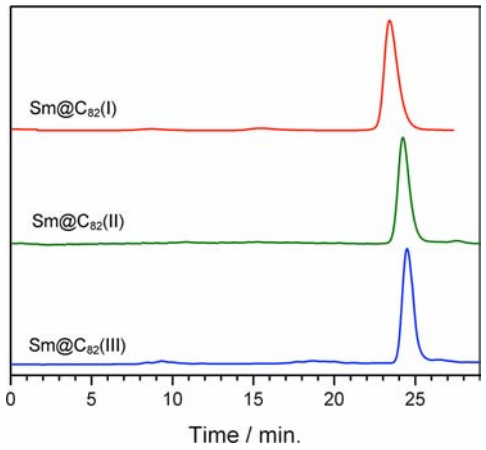

Figure 1. Chromatograms of the purified $Sm@C_{82}$ isomers on a Buckyprep column. HPLC conditions: flow rate, 4.0 mL/min; detection wavelength, 450 nm; eluent, toluene.

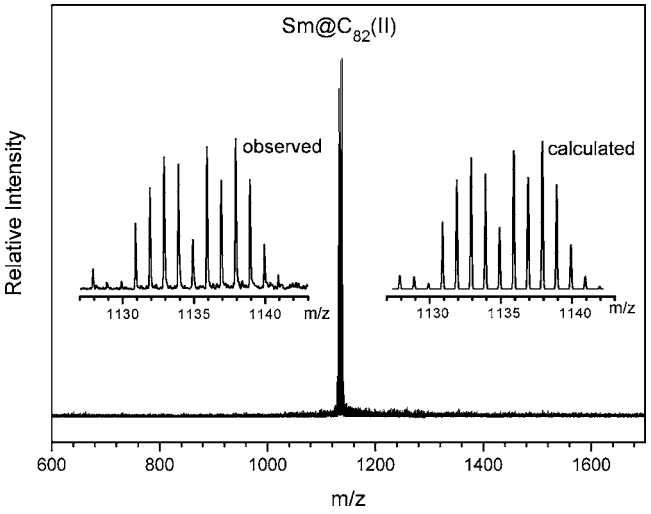

Figure 2. LDI-TOF mass spectrum of a purified sample of $Sm@C_{82}$(II). The insets show expansions of the experimental and theoretical spectra. The mass spectra of the other two isomers are similar and can be found in the Supporting Information.

Figure 2 shows the laser-desorption ionization time-of-flight (LDI-TOF) mass spectrum of $Sm@C_{82}$(II). The insets show expansion of the parent ion peaks and the spectrum computed on the basis of isotope abundances. The mass spectra for the other two isomers are nearly identical as can be seen in the Supporting Information. The UV−vis−NIR absorption spectra of the individual isomers are shown in Figure 3. $Sm@C_{82}$(I) has the lowest energy onset of absorption at 1648 nm and absorption maxima at 1478, 1224, 486, 786, and 465 nm. $Sm@C_{82}$(II) has its onset of absorption at 1295 nm, which is the highest energy for these isomers, and absorption maxima at 1202, 926, 661, 527s, and 496 nm. For $Sm@C_{82}$(III), the onset of absorption is 1402 nm, and there are absorption maxima at 1205, 1037, 887s, 780, 669, and 610s nm.

Crystallographic Characterization of $Sm@C_{3v}(7)\text{-}C_{82}$. Black crystals of $Sm@C_{3v}(7)\text{-}C_{82}\cdot Ni(OEP)\cdot 2$toluene were

dx.doi.org/10.1021/ja304867j | J. Am. Chem. Soc. 2012, 134, 14127−14136

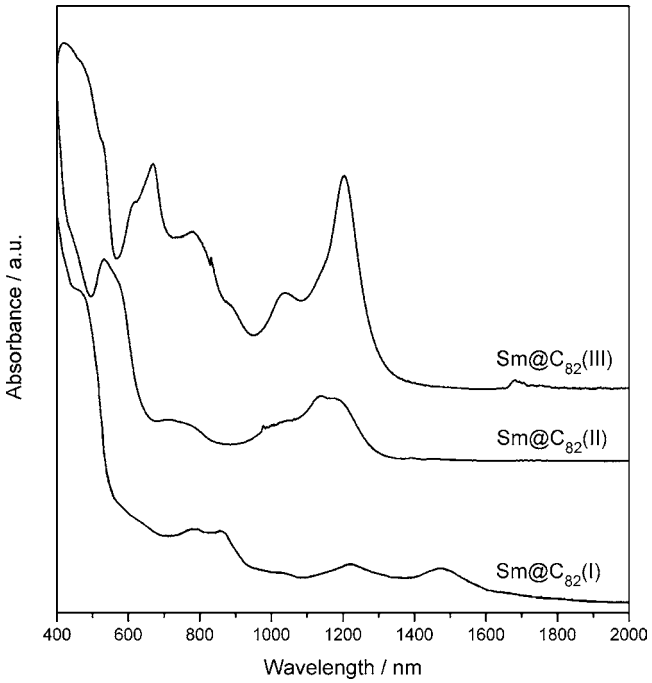

Figure 3. UV−vis−NIR absorption spectra from carbon disulfide solutions of the purified isomers of Sm@C_{82}.

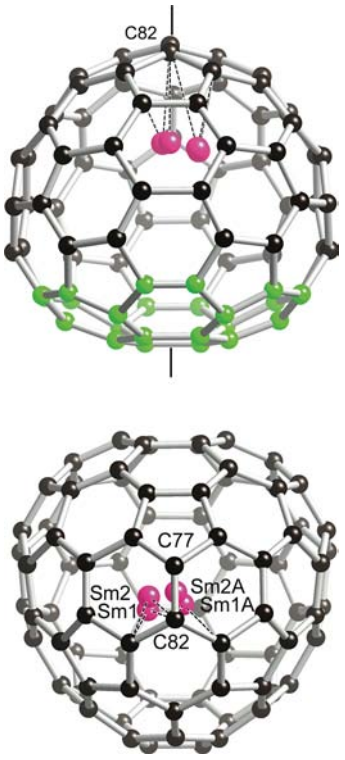

Figure 4. Two views of Sm@C_{3v}(7)-C_{82} from the crystallographic study of Sm@C_{3v}(7)-C_{82}·Ni(OEP)·2toluene. In the upper view, the carbon atoms in the coronene fragment are shown in green, and the vertical line indicates the location of the C_3 axis. These drawings show the two major samarium sites with fractional occupancies of 0.23 along with their crystal-symmetry-generated counterparts, Sm1A and Sm2A.

obtained by layering a toluene solution of Sm@C_{82}(II) over a toluene solution of Ni(OEP). This cocrystallization process was used to obtain crystals with sufficient order so that single-crystal X-ray diffraction data could be obtained and analyzed.[35] Figure 4 shows two drawings of the structure of Sm@C_{3v}(7)-C_{82}. In the upper part, the molecule is aligned so that the C_3 axis, which passes through C82 and the hexagon opposite C82, is vertical. In the lower view, the C_3 axis passes through C82 and the center of the hexagon immediately behind C77. The C_3 axis in C_{3v}(7)-C_{82} passes through the center of a coronene patch, which is shown in Scheme 1. This patch is a distinguishing feature of the C_{3v}(7)-C_{82} cage. The other C_{3v} isomer of C_{82} lacks this patch, but has a sumanene patch in a similar location with the C_3 axis passing through its center. The hydrocarbon coronene is a planar molecule, and incorporation of a coronene patch into a fullerene must incur some strain within the molecule. Previously, the empty cage fullerene, C_s(16)-C_{86}, was isolated and shown to contain a coronene patch within its carbon network.[36]

Figure 5 shows the relative dispositions of the Sm@C_{3v}(7)-C_{82} molecule and the nickel porphyrin. As is usual in such structures, all eight of the ethyl groups of Ni(OEP) embrace the fullerene cage. The coronene patch of Sm@C_{3v}(7)-C_{82} is situated closest to the Ni(OEP) porphyrin plane.

The position of the samarium ion within the fullerene cage is disordered. There are four crystallographic sites for the samarium ion with occupancies of 0.23 for Sm1, 0.23 for Sm2, 0.02 for Sm3, and 0.02 for Sm4. Only the two major sites and the two equivalent sites generated by the crystallographic mirror plane are shown in Figures 4 and 5. These sites cluster about the C_3 axis of the fullerene and are located on the opposite side of the cage from the coronene patch. The closest contacts of the samarium ion and the carbon cage are as follow (Å): Sm1−C81, 2.533(5); Sm2−C80, 2.520(3); Sm1A−C82, 2.555(5); and Sm2A−C82, 2.552(5).

Scheme 1. Coronene and Sumanene Patches

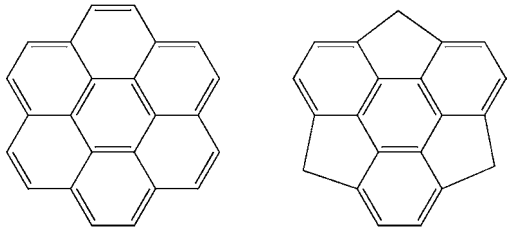

Crystallographic Characterization of Sm@C_s(6)-C_{82}. Black crystals of 0.6667 Sm@C_{3v}(7)-C_{82}/0.3333Sm@C_s(6)-C_{82}·Ni(OEP)·2toluene were obtained by layering a toluene solution of Sm@C_{82}(I) over a toluene solution of Ni(OEP). The sample of Sm@C_{82}(I) used in this particular crystallization effort came from a purification effort that did not produce adequate separation of isomers I and II. Subsequently, we were able to obtain samples of Sm@C_{82}(I) with better isomeric purity, but these samples did not yield crystals that produced any improved X-ray diffraction data. We collected five different data sets on various crystals. The solutions we obtained for these all indicated that the Sm@C_s(6)-C_{82} isomer was present. Here, we report the best structure we obtained.

Crystals of 0.6667 Sm@C_{3v}(7)-C_{82}/0.3333Sm@C_s(6)-C_{82}·Ni(OEP)·2toluene are isostructural with those of Sm@C_{3v}(7)-C_{82}·Ni(OEP)·2toluene. The structures of the two fullerene cages are closely related. Figure 6 shows a drawing that illustrates how the two molecules are interrelated. The

dx.doi.org/10.1021/ja304867j | J. Am. Chem. Soc. 2012, 134, 14127−14136

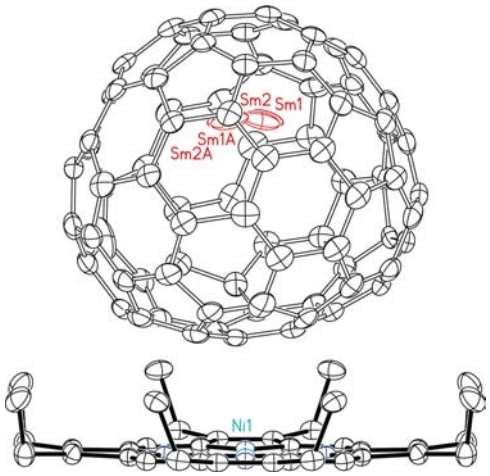

Figure 5. Relative orientations of Sm@C_{3v}(7)-C_{82} and the porphyrin in Sm@C_{3v}(7)-C_{82}·Ni(OEP)·2toluene with 30% thermal ellipsoids. This drawing shows the two major samarium sites with fractional occupancies of 0.23 along with their crystal-symmetry-generated counterparts, Sm1A and Sm2A. The toluene molecules are not shown.

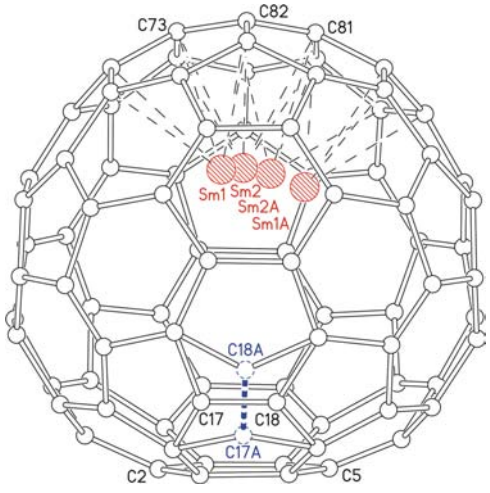

Figure 6. Two views of the fullerene cage(s) in 0.6667 Sm@C_{3v}(7)-C_{82}/0.3333 Sm@C_s(6)-C_{82}·Ni(OEP)·2toluene. The cage for Sm@C_{3v}(7)-C_{82} involves C17 and C18, while C17A and C18A are absent. The cage for Sm@C_s(6)-C_{82} involves C17A and C18A, while for this isomer C17 and C18 are absent. These drawings show the two major samarium sites with fractional occupancies of 0.30 and 0.28 along with their crystal-symmetry-generated counterparts, Sm1A and Sm2A.

fullerene cages C_s(6)-C_{82} and C_{3v}(7)-C_{82} may be transformed into one another by a single Stone–Wales operation, which interchanges the locations of two carbon atoms within the fullerene as shown in Scheme 2. Thus, in Figure 6, the C_{3v}(7)-C_{82} cage is formed by the 82 black carbon atoms. The two blue atoms, C17A and C18A, are not used to form this isomer. The C_s(6)-C_{82} cage is formed by 80 of the black carbon atoms and the two blue carbon atoms, C17A and C18A. In this cage, C17 and C18 are not present. The occupancies of these two pairs of sites were initially refined and then fixed at 0.6667/0.3333. The cocrystallization of closely related fullerene cages at a common site has been observed previously in the structure of (η^2-D_{2d}(23)-C_{84})Ir(CO)Cl(PPh_3)$_2$, where the D_2(22)-C_{84} isomer is also present.[37] The isomers D_{2d}(23)-C_{84} and D_2(22)-C_{84} are related by a single Stone–Wales transformation. Similarly, crystalline C_s(16)-C_{86}/C_2(17)-C_{86}·Ni(OEP)·2toluene contains

Scheme 2. Stone–Wales Transformation and Isomerization Paths

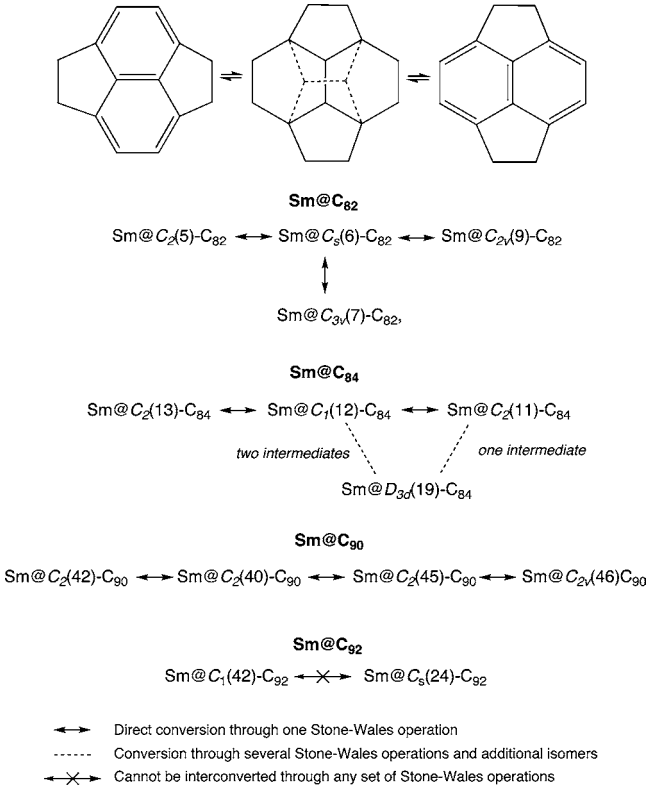

two isomers of C_{86} in a common site.[38] These isomers are interconverted by a Stone–Wales transformation.

Crystallographic Characterization of Sm@C_2(5)-C_{82}. Black crystals of Sm@C_2(5)-C_{82}·Ni(OEP)·2benzene were obtained by layering a benzene solution of Sm@C_{82}(III) over a benzene solution of Ni(OEP). Three drawings of the structure of Sm@C_2(5)-C_{82} are shown in Figure 7. In the top drawing, the C_2 axis is vertical. The middle drawing is oriented so that the viewer looks down the C_2 axis, which passes through the top hexagonal ring and through the midpoint of a C–C bond on the opposite side. Figure 8 shows the relative orientations of Sm@C_2(5)-C_{82} and the porphyrin in Sm@C_2(5)-C_{82}·Ni(OEP)·2benzene.

There is disorder in the location of the samarium ion. There are six samarium ion positions with occupancies of 0.25 for Sm1, 0.09 for Sm2, 0.06 for Sm3, 0.06 for Sm4, 0.06 for Sm5, and 0.01 for Sm6. Because there are two orientations of the C_{82} cage, there are two rather different positions for the major samarium site within the cage. In one orientation shown in (A) and (B) of Figure 7, the major samarium site is located under the hexagonal ring that is bisected by the C_2 axis and lies near that C_2 axis. The second location is shown in part (C) of Figure 7. Crystallographically, there is no way to determine whether either or both of these two locations are occupied. However, computational studies, vide infra, reveal that the site shown in (A) and (B) of Figure 7 lies at an energy minimum, while the site shown in (C) does not. At the site shown in (A) and (B) of Figure 7, the Sm1–C distances to the closest hexagon range from 2.596(7) to 2.783(8) Å.

Computational Studies of the Relative Stabilities of the Sm@C_{82} Isomers. To examine the stabilities and electronic structures of the Sm@C_{82} isomers, geometric

dx.doi.org/10.1021/ja304867j | J. Am. Chem. Soc. 2012, 134, 14127–14136

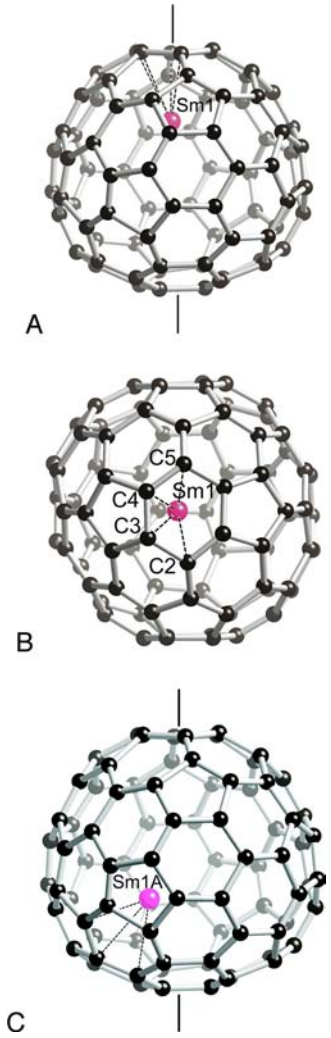

Figure 7. Three views of Sm@$C_2(5)$-C_{82} from the crystallographic study of Sm@$C_2(5)$-C_{82}·Ni(OEP)·2benzene. (A) and (B) show orthogonal views with the samarium in site Sm1. (C) shows a drawing with the samarium in the mirror-related site Sm1A. The C_2 axis of the fullerene is aligned vertically in (A) and (C).

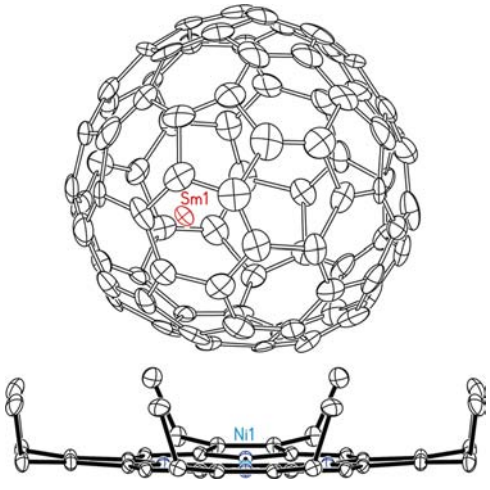

Figure 8. Relative orientations of Sm@$C_2(5)$-C_{82} and the porphyrin in Sm@$C_2(5)$-C_{82}·Ni(OEP)·2benzene with 30% thermal ellipsoids. Only one orientation of the major samarium site is shown. The benzene molecules are not shown.

optimizations using DFT methodology were conducted for all nine IPR isomers. The results in terms of the relative energy, HOMO−LUMO gap, atomic charge, and spin density on Sm are presented in Table 1. These calculations indicate that Sm@$C_2(5)$-C_{82} is the most stable isomer, but that the Sm@$C_{2v}(9)$-C_{82}, Sm@$C_s(6)$-C_{82}, and Sm@$C_{3v}(7)$-C_{82} isomers are relatively close in energy. Sm@$C_{3v}(7)$-C_{82} and Sm@$C_2(5)$-C_{82} have larger HOMO−LUMO gaps than the other two low-energy isomers.

As noted above, the electronic distribution for samarium-containing endohedral fullerenes may be represented by the ionic model, $Sm^{2+}@(C_{2n})^{2-}$, with the cage acquiring two electrons from the interior metal atom. Consequently, calculations were also performed to determine the relative stabilities of the dianions of the nine IPR isomers of C_{82}. Those relative stabilities are listed in Table SI-1 (see the Supporting Information). Figures 9, 10, and 11 show the molecular orbital energies of the neutral, di-, tri-, and tetra-anionic forms of the empty cage isomers, $C_{3v}(7)$-C_{82}, $C_s(6)$-C_{82}, and $C_2(5)$-C_{82}, obtained through DFT methods. These computations show that the HOMO−LUMO gaps are maximized at the dianionic and trianionic stages for $C_2(5)$-C_{82} and $C_s(6)$-C_{82}, while the neutral molecule has the largest HOMO−LUMO gap for $C_{3v}(7)$-C_{82} with triplet ground state of electronic structure.

The computed structures and spin distributions in the Sm@$C_{3v}(7)$-C_{82}, Sm@$C_s(6)$-C_{82}, and Sm@$C_2(5)$-C_{82} are shown in Figure 12. As expected, the spin density is largely localized on the samarium ion. However, very minor amounts of opposite spin are transferred to some of the nearby carbon atoms of the fullerene cage. Notice that for Sm@$C_2(5)$-C_{82} these computations place the samarium ion in a position that corresponds to the site shown in (A) and (B) of Figure 7.

The relationship between the endohedrals and Ni(OEP) molecules appeared in many cases to favor placement of relatively flat regions of the fullerene with the porphyrin, but some notable exceptions have recently appeared: for example, $La_2@D_5(450)$-C_{100} where the curved poles of the fullerene are closest to the porphyrin.[39] Consequently, we have begun to seek other factors that might influence the relationship between the fullerenes and the porphyrins. Figure 13 compares plots of the electrostatic potential in terms of total electron density for Sm@$C_{3v}(7)$-C_{82}, Sm@$C_s(6)$-C_{82}, and Sm@$C_2(5)$-C_{82}. These plots show the portion of each cage that faces the Ni(OEP) molecule. The red arrows point to the carbon atoms closest to the nickel atoms in each crystal. The blue-green color in the regions close to the porphyrin indicates regions of significant positive potential on the endohedral fullerene. In contrast, the regions of the porphyrin that are closest to the fullerene display negative potential in the vicinity of the four nitrogen atoms.[40] Similar arrangements that place regions of positive potential on the fullerene near regions of negative potential on the porphyrin have been reported previously for empty cage fullerenes such as $D_{5h}(1)$-C_{90}[34] and for endohedral fullerenes such as Sm@$C_1(42)$-C_{92}.[41] These electrostatic interactions appear to be significant in producing some degree of orientational order in the cocrystals used for X-ray diffraction.

■ DISCUSSION

This work has described the isolation of three isomers of Sm@C_{82} and the first structural characterization by X-ray diffraction of three $M^{2+}@(C_{2n})^{2-}$ type endohedral fullerenes: Sm@$C_{3v}(7)$-C_{82}, Sm@$C_s(6)$-C_{82}, and Sm@$C_2(5)$-C_{82}. The two cage isomers, Sm@$C_{3v}(7)$-C_{82} and Sm@$C_2(5)$-C_{82}, have not yet

dx.doi.org/10.1021/ja304867j | J. Am. Chem. Soc. 2012, 134, 14127−14136

Table 1. Relative Energies (ΔE, kcal mol^{-1}), HOMO−LUMO Gaps (in eV), Ground State, Atomic Charge, and Spin Density of Sm@C_{82} Isomers[a]

isomer	ΔE (kcal mol^{-1})	HOMO−LUMO gap (eV)	ground state	atomic charge on Sm	spin density on Sm
Sm@C_2(5)-C_{82}	0.00	1.67	^{7}A	1.68	6.03
Sm@C_{2v}(9)-C_{82}	0.64	1.46	^{7}B$_1$	1.68	6.03
Sm@C_s(6)-C_{82}	1.67	1.44	^{7}A″	1.68	6.03
Sm@C_{3v}(7)-C_{82}	3.31	2.05	^{7}A″	1.68	6.03
Sm@C_{3v}(8)-C_{82}	8.33	1.14	^{7}A	1.69	6.02
Sm@C_s(4)-C_{82}	12.90	1.31	^{7}A′	1.68	6.03
Sm@C_2(1)-C_{82}	19.48	1.61	^{7}A	1.66	6.03
Sm@C_2(3)-C_{82}	22.49	1.22	^{7}B	1.66	6.03
Sm@C_s(2)-C_{82}	29.82	0.90	^{7}A″	1.68	6.02

[a]Geometries optimized at the B3LYP level with a 3-21g basis set for carbon and a cep-31g basis set for samarium.

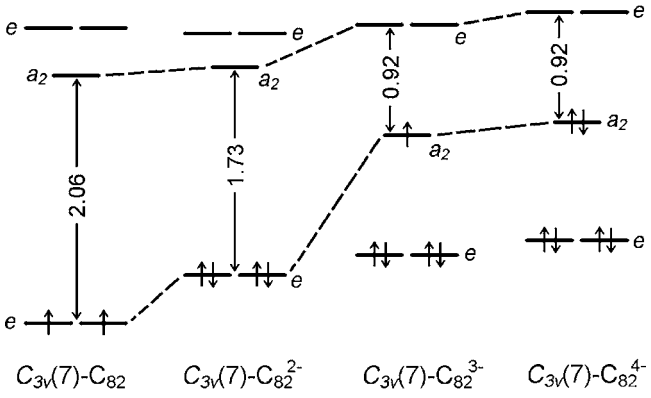

Figure 9. Molecular orbital energy levels (in eV) for the neutral form as well as di-, tri-, and tetra-anions of the empty C_{3v}(7)-C_{82} molecule. The calculations were conducted at the B3LYP/6-31G(d) level.

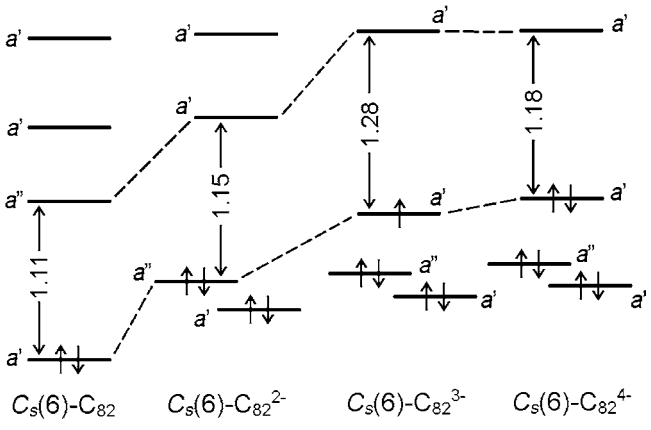

Figure 10. Molecular orbital energy levels (in eV) for the neutral form as well as di-, tri-, and tetra-anions of the empty C_s(6)-C_{82} molecule. The calculations were conducted at the B3LYP/6-31G(d) level.

been observed for any soluble form of the $M^{3+}@(C_{2n})^{3-}$ type endohedral fullerenes such as La@C_{82}. However, endohedral fullerenes that are otherwise insoluble can be extracted with 1,2,4-trichlorobenzene from arc-generated carbon soot.[42,43] During the extraction, reactive dichlorophenyl radicals are formed, and these radicals add to the endohedral fullerenes to form covalent adducts. In this fashion, two dichlorophenyl adducts of the otherwise insoluble La@C_{3v}(7)-C_{82} have been formed and isolated.[44] As noted in the introduction, an analogue of Sm@C_s(6)-C_{82}, La@C_s(6)-C_{82}, has been characterized through ^{13}C NMR spectroscopic measurements.[25]

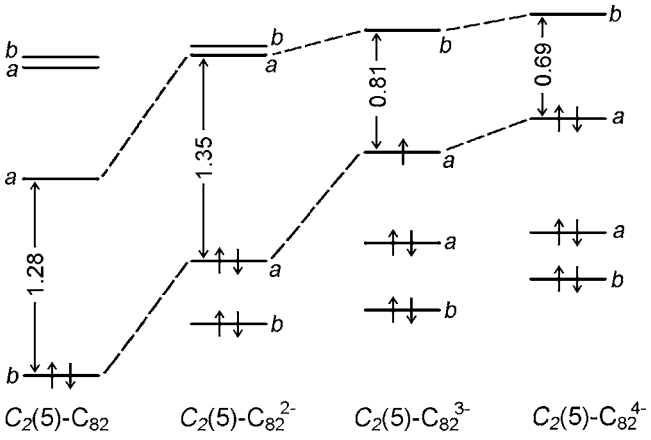

Figure 11. Molecular orbital energy levels (in eV) for the neutral form as well as di-, tri-, and tetra-anions of the empty C_2(5)-C_{82} molecule. The calculations were conducted at the B3LYP/6-31G(d) level.

It is useful to consider the relationships between the compounds reported here and other endohedral fullerenes of the $M^{2+}@(C_{2n})^{2-}$ type. Because the UV−vis−NIR spectra of endohedral fullerenes reflect the cage structure and charge distribution, it is possible to correlate information on a variety of related endohedrals. Table 2 provides information from several studies on isomers of Sm@C_{82}, Eu@C_{82}, Tm@C_{82}, Yb@C_{82}, and Ca@C_{82}. The rows in this table show the individual isomers identified in different laboratories, along with appropriate references. The columns each contain compounds with similar UV−vis−NIR spectra. Where there is overlap, the results obtained by X-ray diffraction on Sm@C_{82} isomers agree with the structural assessments obtained from the ^{13}C NMR studies. Thus, Sm@C_{82}(III) and Yb@C_{82}(II) have similar UV−vis−NIR spectra and contain the C_2(5)-C_{82} cage as shown by crystallography and ^{13}C NMR spectroscopy, respectively.[29] Additionally, a previous ^{13}C NMR study showed that the fullerene cage in Ca@C_{82}(II) was one of two C_{3v} isomers.[26] Now we can infer that Ca@C_{82}(II) is Ca@C_{3v}(7)-C_{82}, based on the UV−vis−NIR spectral similarity to crystallographically characterized Sm@C_{3v}(7)-C_{82}.

In regard to the Sm@C_{82} isomers, it appears that the three studies reporting their isolation have produced five individual isomers, although a different set of isomers was produced in each laboratory. Liu *et al.* produced four isomers denoted Sm@C_{82}(I^L) to Sm@C_{82}(IV^L).[29] Their isomer Sm@C_{82}(I^L) was not produced in either of the other two studies on Sm@C_{82} isomers. Its structure remains unknown. Okazaki *et al.* isolated

dx.doi.org/10.1021/ja304867j | J. Am. Chem. Soc. 2012, 134, 14127−14136

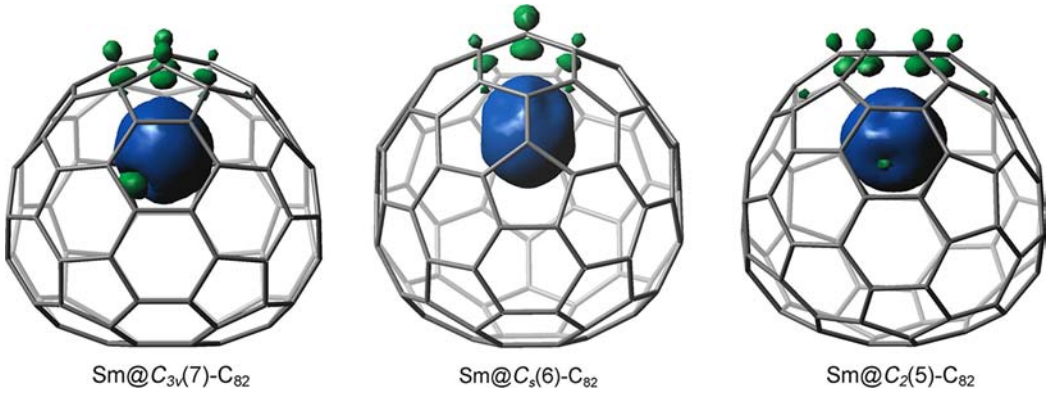

Figure 12. Computed structures and spin density distribution in Sm@C_{3v}(7)-C_{82}, Sm@C_s(6)-C_{82}, and Sm@C_2(5)-C_{82} at the isovalue of 0.0005 e/bohr^3.

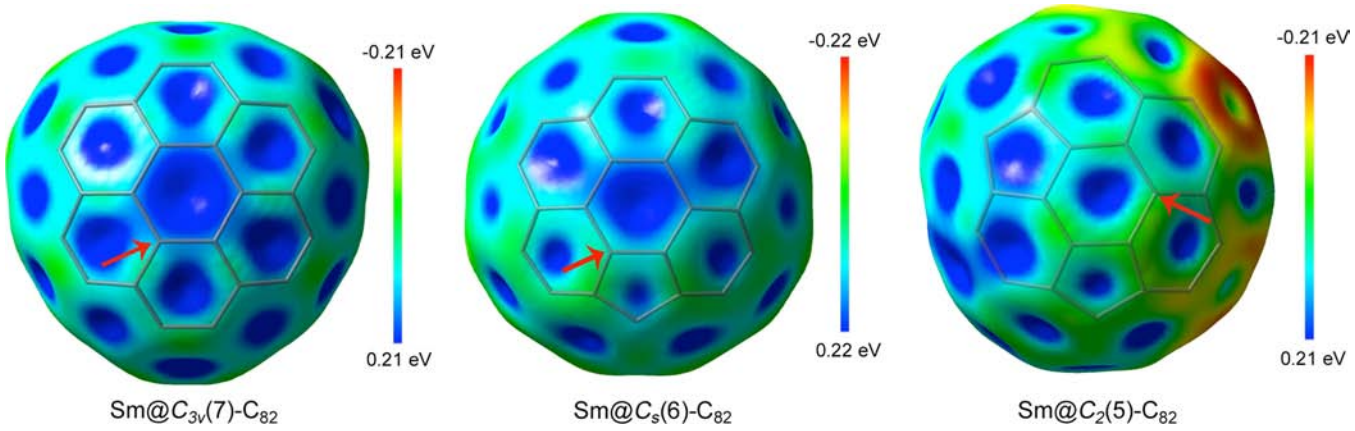

Figure 13. Plots of electrostatic potential (in eV) in terms of total electron density (0.001 e/bohr^3) mapped on the isosurface facing the Ni(OEP) molecule for the three isomers of Sm@C_{82}. Two-dimensional projections of the bonds onto the plots are also shown for clarity. The red arrows indicate the carbon atoms nearest the nickel ion.

Table 2. Classification of the Structures of $M^{2+}@(C_{82})^{2-}$ Isomers on the Basis of Similarities of UV−Vis−NIR Spectra

	cage symmetry				
ref	unknown	C_s(6)-C_{82}	C_{3v}(7)-C_{82}	C_2(5)-C_{82}	C_{2v}(9)-C_{82}
this work		Sm@C_{82}(I)[a]	Sm@C_{82}(II)[a]	Sm@C_{82}(III)[a]	
32	Sm@C_{82}(I^L)	Sm@C_{82}(II^L)		Sm@C_{82}(III^L)	Sm@C_{82}(IV^L)
30		Sm@C_{82}(I^O)		Sm@C_{82}(II^O)	Sm@C_{82}(III^O)
62		Eu@C_{82}(I)		Eu@C_{82}(II)	Eu@C_{82}(III)
63		Tm@C_{82}(I)[b]		Tm@C_{82}(II)[b]	Tm@C_{82}(III)[b]
64		Tm@C_{82}(B)		Tm@C_{82}(A)	Tm@C_{82}(C)
29		Yb@C_{82}(I)[b]		Yb@C_{82}(II)[b]	Yb@C_{82}(III)[b]
65		Yb@C_{82}(I)		Yb@C_{82}(II)	Yb@C_{82}(III)
26		Ca@C_{82}(I)	Ca@C_{82}(II)	Ca@C_{82}(III)	Ca@C_{82}(IV)
27		Ca@C_{82}(I)	Ca@C_{82}(II)	Ca@C_{82}(III), Sr@C_{82}, Ba@C_{82}	Ca@C_{82}(IV)
28		Ca@C_{82}(I)[c]	Ca@C_{82}(II)[c]	Ca@C_{82}(III)[c]	Ca@C_{82}(IV)[c]

[a]Structure determined by single-crystal X-ray diffraction, this work. [b]Structure determined by ^{13}C NMR spectroscopy and DFT computation. [c]Structure determined by ^{13}C NMR spectroscopy.

three isomers denoted as Sm@C_{82}(I^O), etc.[30,31] The UV−vis−NIR spectrum of our Sm@C_{82}(I) corresponds to the spectra of Sm@C_{82}(II^L) and Sm@C_{82}(I^O). Our Sm@C_{82}(II), which is Sm@C_{3v}(7)-C_{82}, was not observed by Liu *et al.* or by Okazaki *et al.* The spectra of our Sm@C_{82}(III) (which is Sm@C_2(5)-C_{82}), Sm@C_{82}(III^L), and Sm@C_{82}(II^O) are similar to the spectrum of Yb@C_{82}(II), which has been identified as Yb@C_2(5)-C_{82} by ^{13}C NMR spectroscopy. Likewise, the spectra of Sm@C_{82}(IV^L) and Sm@C_{82}(III^O) are similar to the spectrum of Yb@C_{82}(III), which has been identified as Yb@C_{2v}(9)-C_{82}, again by ^{13}C NMR spectroscopy.

The different distributions of Sm@C_{82} isomers produced in three different laboratories appear to reflect differences in the methods of fullerene formation. In particular, the source of the samarium used in these laboratories differed. In our laboratory, hollow graphite rods were doped with Sm_2O_3 and graphite powder. Okazaki *et al.* used a mixture of graphite powder, silicon carbide, and Sm_2Co_{17} alloy as their samarium

dx.doi.org/10.1021/ja304867j | J. Am. Chem. Soc. 2012, 134, 14127−14136

Table 3. Crystal Data and Data Collection Parameters

	$Sm@C_{3v}(7)$-C_{82}·Ni(OEP)·2toluene	0.6667$Sm@C_{3v}(7)$-C_{82}/0.3333$Sm@C_s(6)$-C_{82}·Ni(OEP)·2toluene	$Sm@C_2(5)$-C_{82}·Ni(OEP)·2benzene
isomer	$Sm@C_{82}$(II)	impure Sm(I)	$Sm@C_{82}$(III)
formula	$C_{132}H_{60}N_4NiSm$	$C_{132}H_{60}N_4NiSm$	$C_{130}H_{56}N_4NiSm$
fw	1910.90	1910.90	1882.85
color, habit	black block	black block	black block
crystal system	monoclinic	monoclinic	monoclinic
space group	*C*2/*m*	*C*2/*m*	*C*2/*m*
a, Å	25.2726(8)	25.3373(11)	25.3364(4)
b, Å	14.9311(5)	14.8267(11)	15.0718(2)
c, Å	20.3162(6)	20.4311(11)	19.7948(3)
β, deg	96.892(2)	97.050(2)	94.208(4)
V, Å^3	7610.9(4)	7617.3(8)	7538.57(19)
Z	4	4	4
T (K)	90(2)	90(2)	90(2)
radiation (*λ*, Å)	synchrotron 0.77490	Mo K*α* 0.71073	Mo K*α* 0.71073
unique data	17 239 [*R*(int) = 0.0303]	12 552 [*R*(int) = 0.0351]	14 174 [*R*(int) = 0.0245]
parameters	1055	1102	1098
restraints	0	1065	2752
obsd ($I > 2\sigma(I)$) data	14 816	10 309	11 674
R1[a] (obsd data)	0.0495	0.0690	0.0678
wR2[b] (all data)	0. 1276	0.1607	0.2036

[a]For data with $I > 2\sigma I$, R1 = $(\sum||F_o| - |F_c||)/(\sum|F_o|)$. [b]For all data, wR2 = $(\sum[w(F_o^2 - F_c^2)^2])/(\sum[w(F_O^2)^2])$.

source.[30,31] Liu *et al.* used $SmNi_2$ alloy mixed with graphite powder to produce their samarium endohedrals.[29] Previously, we noted that these same three laboratories produced different sets of $Sm@C_{84}$ isomers, and we again attributed the variations in isomers produced to the different samarium sources involved.[45] The relative yields of different isomers are likely controlled by the method of formation rather than solely thermodynamic considerations. There are other studies that also suggest that chemical additives influence the pattern of fullerenes that are produced during the electric arc generation of fullerenes.[46,47]

As shown in Scheme 2, the Stone–Wales transformation provides a means of isomerization of a fullerene though rotation of a single C_2 unit.[10] All of the nine IPR-obeying C_{82} cages lie on a single interconversion map, which shows the path of isomerization of fullerenes that are possible through Stone–Wales transformations. Consequently, the four isomers of $Sm@C_{82}$ whose structures are reasonably well established can be interconverted through Stone–Wales transformations. As Scheme 2 indicates, $Sm@C_s(6)$-C_{82} can be converted into any one of the other three isomers ($Sm@C_2(5)$-C_{82}, $Sm@C_{3v}(7)$-C_{82}, and $Sm@C_{2v}(9)$-C_{82}) through a single Stone–Wales transformation. Similarly, the structurally characterized isomers of $Sm@C_{84}$[48] and $Sm@C_{90}$ are also related to one another through Stone–Wales transformations. However, the two known isomers of $Sm@C_{92}$ are not related by such interconversions. Stone–Wales transformations may be occurring during the process of fullerene formation and may be responsible as paths to allow particular isomers to form and possibly equilibrate. Note that the isomerization of C_{78} has been observed in the gas phase at ca. 1000 K.[49] However, the formation of the two known isomers of $Sm@C_{92}$, which are not connected through Stone–Wales isomerization, indicates that a Stone–Wales transformation path is not necessary to produce these particular isomers.

The positioning of the metal ions inside the C_{82} cage isomers has been at times a somewhat contentious issue. For the molecules we have structurally identified, the positioning of the samarium ions is rather clearly established. For $Sm@C_{3v}(7)$-C_{82}, the samarium sites cluster near the 3-fold symmetry axis and are well away from the coronene portion of the molecule. In the case of $Sm@C_2(5)$-C_{82}, the computational results suggest that the samarium ion occupies a site below a hexagon and near the 2-fold axis of the cage, that is, the crystallographic site shown in (A) and (B) of Figure 6. For the highly studied $La@C_{2v}(9)$-C_{82}, computational and experimental work indicates that the lanthanum ion is similarly positioned beneath a hexagon and near the 2-fold axis.[50−52] However, anomalous metal ion locations have been suggested to occur in the related endohedrals, $Gd@C_{2v}(9)$-C_{82} and $Eu@C_{2v}(9)$-C_{82}.[53,54] In contrast, other studies suggest that these two molecules have a more normal metal ion placement analogous to the situation in $La@C_{2v}(9)$-C_{82}.[55−57]

■ CONCLUSIONS

Three soluble isomers of $Sm@C_{82}$ were obtained from the carbon soot produced by vaporization of hollow carbon rods doped with Sm_2O_3/graphite powder in an electric arc, and the structures of these isomers, $Sm@C_{3v}(7)$-C_{82}, $Sm@C_s(6)$-C_{82}, and $Sm@C_2(5)$-C_{82}, were determined by single-crystal X-ray diffraction. When combined with studies in other laboratories, the structures of four soluble isomers of $Sm@C_{82}$ ($Sm@C_2(5)$-C_{82}, $Sm@C_s(6)$-C_{82}, $Sm@C_{3v}(7)$-C_{82}, and $Sm@C_{2v}(9)$-C_{82}) are reasonably well established.

■ EXPERIMENTAL SECTION

Formation and Isolation of the $Sm@C_{82}$ Isomers. An 8 × 150 mm hollow graphite rod was filled with Sm_2O_3 and graphite powder (Sm:C atomic ratio 1:40) and subsequently vaporized as the anode in DC arc discharge. The raw soot was dissolved in *o*-dichlorobenzene with sonocation for 8 h and then vacuum filtered. After removal of the solvent on a rotary evaporator, the dry extract was dissolved in chlorobenzene. The resulting solution was subjected to a four-stage HPLC isolation process without recycling. Chromatographic details are given in the Supporting Information.

The purity and composition of the samples of isomers of Sm@C_{82} were verified by laser desorption ionization time-of-flight mass spectrometry (LDI-TOF-MS). Ultraviolet−visible−near-infrared (UV−vis−NIR) spectra were obtained through the use of a UV-4100 spectrophotometer (Hitachi High-Technologies Corp.) with samples dissolved in carbon disulfide.

Crystal Structure Determinations. A crystal of Sm@C_{3v}(7)-C_{82}·Ni(OEP)·2toluene was mounted in the nitrogen cold stream provided by an Oxford Cryostream low temperature apparatus on the goniometer head of a Bruker D8 diffractometer equipped with an ApexII CCD detector at the Advanced Light Source, Berkeley, CA, beamline 11.3.1. Data were collected with the use of silicon(111) monochromated synchrotron radiation (λ = 0.77490 Å). Black crystals of Sm@C_2(5)-C_{82}·Ni(OEP)·2benzene and 0.6667 Sm@C_{3v}(7)-C_{82}/0.3333Sm@C_s(6)-C_{82}·Ni(OEP)·2toluene were mounted in the nitrogen cold stream provided by a Cryo Industries low temperature apparatus on the goniometer head of a Bruker SMART diffractometer equipped with an ApexII CCD detector. Data were collected with the use of MoKα radiation (λ = 0.71073 Å). Crystal data are given in Table 3. The structures were solved by direct methods (SHELXS97) and refined by full-matrix least-squares on F^2 (SHELXL97).[58]

The crystals of Sm@C_{3v}(7)-C_{82}·Ni(OEP)·2toluene and 0.6667Sm@C_{3v}(7)-C_{82}/0.3333Sm@C_s(6)-C_{82}·Ni(OEP)·2toluene show disorder in the orientation of the C_{82} molecule. Carbon atoms C40, C71, and C78 reside on the mirror plane. The remaining 79 carbons were refined at 0.5 occupancy. There are two molecules of toluene that are disordered with respect to crystallographic mirror planes. There is disorder in the Sm positions; occupancies were initially refined and then fixed. The occupancies for Sm@C_{3v}(7)-C_{82}·Ni(OEP)·2toluene, which sum to 0.5, are Sm1, 0.23; Sm2, 0.23; Sm3, 0.02; and Sm4, 0.02. Only Sm1 and Sm2 were refined with anisotropic thermal parameters.

There are two orientations of the C_{82} molecule in the structure of Sm@C_2(5)-C_{82}·Ni(OEP)·2benzene. Both are disordered with respect to the crystallographic mirror plane. The major orientation (occupancy of 0.447) was refined with anisotropic thermal parameters. The minor orientation of the C_{82} cage was refined as a rigid group, whose structure was based on the geometry found for the major orientation. One of the benzene solvate molecules is disordered and was refined in two orientations. There are six Sm positions with occupancies ranging from 0.25 to 0.01 (Sm1, 0.25; Sm2, 0.09; Sm3, 0.06; Sm4, 0.06; Sm5, 0.06; Sm6, 0.01); the occupancy sum is 0.50000. Only Sm1, Sm2, Sm3, and Sm4 were refined with anisotropic thermal parameters.

Computational Details. Geometries of the nine isomers of Sm@C_{82} were fully optimized by nonlocal density functional calculations at the B3LYP level.[59] The effective core potential and basis set developed by Stevens *et al.* were used for samarium (CEP-31g),[60] and the split-valence 3-21G basis set was used for carbon. All calculations were carried out with the Gaussian 03 program.[61]

■ ASSOCIATED CONTENT

Supporting Information

Complete citation for ref 61, preparative details, and computational results; X-ray crystallographic files in CIF format for Sm@C_{3v}(7)-C_{82}·Ni(OEP)·2toluene, 0.6667 Sm@C_{3v}(7)-C_{82}/0.3333 Sm@C_s(6)-C_{82}·Ni(OEP)·2toluene, and Sm@C_2(5)-C_{82}·Ni(OEP)·2benzene. This material is available free of charge via the Internet at http://pubs.acs.org.

■ AUTHOR INFORMATION

Corresponding Author

zyliu@zju.edu.cn; mmolmstead@ucdavis.edu; albalch@ucdavis.edu

Notes

The authors declare no competing financial interest.

■ ACKNOWLEDGMENTS

We thank the U.S. National Science Foundation [Grants CHE-1011760 and CHE-0716843 to A.L.B. and M.M.O.], the U.S. Department of Education for a GAANN fellowship to B.Q.M., the National Natural Science Foundation of China [11179039, 20971108], the National Basic Research Program of China [2011CB808200], the Zhejiang Provincial Natural Science Foundation of China [LR12B01001], and the Advanced Light Source, Lawrence Berkeley Laboratory, for support. The Advanced Light Source is supported by the Director, Office of Science, Office of Basic Energy Sciences, of the U.S. Department of Energy under Contract No. DE-AC02-05CH11231.

■ REFERENCES

(1) Chaur, M. N.; Melin, F.; Ortiz, A. L.; Echegoyen, L. *Angew. Chem., Int. Ed.* **2009**, *48*, 7514−7538.
(2) Lu, X.; Akasaka, T.; Nagase, S. *Chem. Commun.* **2011**, *47*, 5942−5957.
(3) Mikawa, M.; Kato, H.; Okumura, M.; Narazaki, M.; Kanazawa, Y.; Miwa, N.; Shinohara, H. *Bioconjugate Chem.* **2001**, *12*, 510−514.
(4) Bolskar, R. D.; Benedetto, A. F.; Husebo, L. O.; Price, R. E.; Jackson, E. F.; Wallace, S.; Wilson, L. J.; Alford, J. M. *J. Am. Chem. Soc.* **2003**, *125*, 5471−5478.
(5) Shultz, M. D.; Duchamp, J. C.; Wilson, J. D.; Shu, C.-Y.; Ge, J.; Zhang, J.; Gibson, H. W.; Fillmore, H. L.; Hirsch, J. I.; Dorn, H. C.; Fatouros, P. P. *J. Am. Chem. Soc.* **2010**, *132*, 4980−4981.
(6) Rodríguez-Fortea, A.; Balch, A. L; Poblet, J. M. *Chem. Soc. Rev.* **2011**, *40*, 3551−3563.
(7) Rodriguez-Fortea, A.; Alegret, N.; Balch, A. L.; Poblet, J. M. *Nat. Chem.* **2010**, *2*, 955−961.
(8) Chai, Y.; Guo, T.; Jin, C. M.; Haufler, R. E.; Chibante, L. P. F.; Fure, J.; Wang, L. H.; Alford, J. M.; Smalley, R. E. *J. Phys. Chem.* **1991**, *95*, 7564−7568.
(9) Maeda, Y.; Tsuchiya, T.; Lu, X.; Takano, Y.; Akasaka, T.; Nagase, S. *Nanoscale* **2011**, *3*, 2421.
(10) Fowler, P. W.; Manolopoulous, D. E. *An Atlas of Fullerenes*; Clarendon: Oxford, 1995.
(11) Mercado, B. Q.; Beavers, C. M.; Olmstead, M. M.; Chaur, M. N.; Walker, K.; Holloway, B. C.; Echegoyen, L.; Balch, A. L. *J. Am. Chem. Soc.* **2008**, *130*, 7854−7855.
(12) Olmstead, M. M.; de Bettencourt-Dias, A.; Stevenson, S.; Dorn, H. C.; Balch, A. L. *J. Am. Chem. Soc.* **2002**, *124*, 4172.
(13) Olmstead, M. M.; Lee, H. M.; Stevenson, S.; Dorn, H. C.; Balch, A. L. *Chem. Commun.* **2002**, 2688−2689.
(14) Valencia, R.; Rodríguez-Fortea, A.; Poblet, J. M. *J. Phys. Chem. A* **2008**, *112*, 4550−4555.
(15) Mercado, B. Q.; Chen, N.; Rodríguez-Fortea, A.; Mackey, M. A.; Stevenson, S.; Echegoyen, L.; Poblet, J. M.; Olmstead, M. M.; Balch, A. L. *J. Am. Chem. Soc.* **2011**, *133*, 6752−6760.
(16) Mercado, B. Q.; Chen, N.; Rodríguez-Fortea, A.; Mackey, M. A.; Stevenson, S.; Echegoyen, L.; Poblet, J. M.; Olmstead, M. M.; Balch, A. L. *J. Am. Chem. Soc.* **2011**, *133*, 6752−6760.
(17) Iiduka, Y.; Wakahara, T.; Nakajima, K.; Nakahodo, T.; Tsuchiya, T.; Maeda, Y.; Akasaka, T.; Yoza, K.; Liu, M. T. H.; Mizorogi, N.; Nagase, S. *Angew. Chem., Int. Ed.* **2007**, *46*, 5562−5564.
(18) Stevenson, S.; Mackey, M. A.; Stuart, M. A.; Phillips, J. P.; Easterling, M. L.; Chancellor, C. J.; Olmstead, M. M.; Balch, A. L. *J. Am. Chem. Soc.* **2008**, *130*, 11844−11845.
(19) Valencia, R.; Rodriguez-Fortea, A.; Stevenson, S.; Balch, A. L.; Poblet, J. M. *Inorg. Chem.* **2009**, *48*, 5957−5961.
(20) Lu, X.; Nakajima, K.; Iiduka, Y.; Nikawa, H.; Mizorogi, N.; Slanina, Z.; Tsuchiya, T.; Nagase, S.; Akasaka, T. *J. Am. Chem. Soc.* **2011**, *133*, 19553−19558.
(21) Akasaka, T.; Wakahara, T.; Nagase, S.; Kobayashi, K.; Waelchli, M.; Yamamoto, K.; Kondo, M.; Shirakura, S.; Okubo, S.; Maeda, Y.; Kato, T.; Kako, M.; Nakadaira, Y.; Nagahata, R.; Gao, X.; Van

Caemelbecke, E.; Kadish, K. M. *J. Am. Chem. Soc.* **2000**, *122*, 9316−9317.
(22) Maeda, Y.; Matsunaga, Y.; Wakahara, T.; Takahashi, S.; Tsuchiya, T.; Ishitsuka, M. O.; Hasegawa, T.; Akasaka, T.; Liu, M. T. H.; Kokura, K.; Horn, E.; Yoza, K.; Kato, T.; Okubo, S.; Kobayashi, K.; Nagase, S.; Yamamoto, K. *J. Am. Chem. Soc.* **2004**, *126*, 6858−6859.
(23) Akasaka, T.; Lu, X.; Kuga, H.; Nikawa, H.; Mizorogi, N.; Slanina, Z.; Tsuchiya, T.; Yoza, K.; Nagase, S. *Angew. Chem., Int. Ed.* **2010**, *49*, 9715−9719.
(24) Sato, S.; Nikawa, H.; Seki, S.; Wang, L.; Luo, G.; Lu, J.; Haranaka, M.; Tsuchiya, T.; Nagase, S.; Akasaka, T. *Angew. Chem., Int. Ed.* **2012**, *51*, 1589−1591.
(25) Akasaka, T.; Wakahara, T.; Nagase, S.; Kobayashi, K.; Waelchli, M.; Yamamoto, K.; Kondo, M.; Shirakura, S.; Maeda, Y.; Kato, T.; Kako, M.; Nakadaira, Y.; Gao, X.; Van Caemelbecke, E.; Kadish, K. M. *J. Phys. Chem. B* **2001**, *105*, 2971−2974.
(26) Xu, Z.; Nakane, T.; Shinohara, H. *J. Am. Chem. Soc.* **1996**, *118*, 11309−11310.
(27) John, T.; Dennis, S.; Shinohara, H. *Appl. Phys. A: Mater. Sci. Process.* **1998**, *66*, 243−247.
(28) Kodama, T.; Fujii, R.; Miyake, Y.; Sakaguchi, K.; Nishikawa, H.; Ikemoto, I.; Kikuchi, K.; Achiba, Y. *Chem. Phys. Lett.* **2003**, *377*, 197−200.
(29) Lu, X.; Slanina, Z.; Akasaka, T.; Tsuchiya, T.; Mizorogi, N.; Nagase, S. *J. Am. Chem. Soc.* **2010**, *132*, 5896−5905.
(30) Okazaki, T.; Lian, Y. F.; Gu, Z. N.; Suenaga, K.; Shinohara, H. *Chem. Phys. Lett.* **2000**, *320*, 435−440.
(31) Okazaki, T.; Suenaga, K.; Lian, Y. F.; Gu, Z. N.; Shinohara, H. *J. Mol. Graphics Modell.* **2001**, *19*, 244−251.
(32) Liu, J.; Shi, Z. J.; Gu, Z. N. *Chem.-Asian J.* **2009**, *4*, 1703−1711.
(33) Sun, D.-Y.; Liu, Z.-Y.; Guo, X.-H.; Xu, W.-G.; Liu, S.-Y. *J. Phys. Chem. B* **1997**, *101*, 3927−3930.
(34) Mercado, B. Q.; Jiang, A.; Yang, H.; Wang, Z.; Jin, H.; Liu, Z.; Olmstead, M. M.; Balch, A. L. *Angew. Chem., Int. Ed.* **2009**, *48*, 9114−9116.
(35) Olmstead, M. M.; Costa, D. A.; Maitra, K.; Noll, B. C.; Phillips, S. L.; Van Calcar, P. M.; Balch, A. L. *J. Am. Chem. Soc.* **1999**, *121*, 7090−7097.
(36) Wang, Z.; Yang, H.; Jiang, A.; Liu, Z.; Olmstead, M. M.; Balch, A. L. *Chem. Commun.* **2010**, *46*, 5262−5264.
(37) Balch, A. L.; Ginwalla, A. S.; Lee, J. W.; Noll, B. C.; Olmstead, M. M. *J. Am. Chem. Soc.* **1994**, *116*, 2227−2228.
(38) Wang, Z.; Yang, H.; Jiang, A.; Liu, Z.; Olmstead, M. M.; Balch, A. L. *Chem. Commun.* **2010**, *46*, 5262−5264.
(39) Beavers, C. M.; Jin, H.; Yang, H.; Wang, Z.; Wang, X.; Ge, H.; Liu, Z.; Mercado, B. Q.; Olmstead, M. M.; Balch, A. L. *J. Am. Chem. Soc.* **2011**, *133*, 15338−15341.
(40) Yang, H.; Beavers, C. M.; Wang, Z.; Jiang, A.; Liu, Z.; Jin, H.; Mercado, B. Q.; Olmstead, M. M.; Balch, A. L. *Angew. Chem., Int. Ed.* **2010**, *49*, 886−890.
(41) Jin, H.; Yang, H.; Meilan, Yu, M.; Liu, Z.; Beavers, C. M.; Olmstead, M. M.; Balch, A. L. *J. Am. Chem. Soc.* **2012**, *134*, 10933−10941.
(42) Nikawa, H.; Kikuchi, T.; Wakahara, T.; Nakahodo, T.; Tsuchiya, T.; Rahman, G. M. A.; Akasaka, T.; Maeda, Y.; Yoza, K.; Horn, E.; Mizorogi, N.; Nagase, S. *J. Am. Chem. Soc.* **2005**, *127*, 9684−9685.
(43) Wakahara, T.; Nikawa, H.; Kikuchi, T.; Nakahodo, T.; Rahman, G. M. A.; Tsuchiya, T.; Maeda, Y.; Akasaka, T.; Yoza, K.; Horn, E.; Yamamoto, K.; Mizorogi, N.; Slanina, Z.; Nagase, S. *J. Am. Chem. Soc.* **2006**, *128*, 14228−14229.
(44) Akasaka, T.; Lu, X.; Kuga, H.; Nikawa, H.; Mizorogi, N.; Slanina, Z.; Tsuchiya, T.; Yoza, K.; Nagase, S. *Angew. Chem., Int. Ed.* **2010**, *49*, 9715−9719.
(45) Yang, H.; Yu, M.; Jin, H.; Liu, Z.; Yao, M.; Liu, B.; Olmstead, M. M.; Balch, A. L. *J. Am. Chem. Soc.* **2012**, *134*, 5331−5338.
(46) Tagmatarchis, N.; Avent, A. G.; Prassides, K.; Dennis, T. J. S.; Shinohara, H. *Chem. Commun.* **1999**, 1023−1024.
(47) Tagmatarchis, N.; Okada, K.; Tomiyama, T.; Yoshida, T.; Kobayashi, Y.; Shinohara, H. *Chem. Commun.* **2001**, 1366−1367.
(48) Yang, H.; Yu, M.; Zhen, Z.; Wang, Z.; Liu, Z.; Beavers, C. M.; Mercado, B. Q.; Olmstead, M. M.; Balch, A. L. *J. Am. Chem. Soc.* **2011**, *133*, 6299−6306.
(49) Cross, J. R.; Saunders, M. *J. Am. Chem. Soc.* **2005**, *127*, 3044−3047.
(50) Kobayashi, K.; Nagase, S. *Chem. Phys. Lett.* **1998**, *282*, 325−329.
(51) Maeda, Y.; Matsunaga, Y.; Wakahara, T.; Takahashi, S.; Tsuchiya, T.; Ishitsuka, M. O.; Hasegawa, T.; Akasaka, T.; Liu, M. T. H.; Kokura, K.; Horn, E.; Yoza, K.; Kato, T.; Okubo, S.; Kobayashi, K.; Nagase, S.; Yamamoto, K. *J. Am. Chem. Soc.* **2004**, *126*, 6858−6859.
(52) Nishibori, E.; Takata, M.; Sakata, M.; Tanaka, H.; Hasegawa, M.; Shinohara, H. *Chem. Phys. Lett.* **2000**, *330*, 497−502.
(53) Nishibori, E.; Iwata, K.; Sakata, M.; Takata, M.; Tanaka, H.; Kato, H.; Shinohara, H. *Phys. Rev. B* **2004**, *69*, 113412-1−113412-4.
(54) Sun, B.-Y.; Sugai, T.; Nishibori, E.; Iwata, K.; Sakata, M.; Takata, M.; Shinohara, H. *Angew. Chem., Int. Ed.* **2005**, *44*, 4568−4571.
(55) Mizorogi, N.; Nagase, S. *Chem. Phys. Lett.* **2006**, *431*, 110−112.
(56) Akasaka, T.; Kono, T.; Takematsu, Y.; Nikawa, H.; Nakahodo, T.; Wakahara, T.; Ishitsuka, M. O.; Tsuchiya, T.; Maeda, Y.; Liu, M. T. H.; Yoza, K.; Kato, T.; Yamamoto, K.; Mizorogi, N.; Slanina, Z.; Nagase, S. *J. Am. Chem. Soc.* **2008**, *130*, 12840−12841.
(57) Suzuki, M.; Lu, X.; Sato, S.; Nikawa, H.; Mizorogi, N.; Slanina, Z.; Tsuchiya, T.; Nagase, S.; Akasaka, T. *Inorg. Chem.* **2012**, *51*, 5270−5273.
(58) Sheldrick, G. M. *Acta Crystallogr.* **2008**, *A64*, 112−122.
(59) (a) Becke, A. D. *Phys. Rev. A* **1988**, *38*, 3098−3100. (b) Lee, C.; Yang, W.; Parr, R. G. *Phys. Rev. B* **1988**, *37*, 785−789.
(60) Stevens, W.; Basch, H.; Krauss, J. *J. Chem. Phys.* **1984**, *81*, 6026−6033.
(61) Frisch, M. J.; *et al. Gaussian 03*, revision C.02; Gaussian, Inc.: Pittsburgh, PA, 2003.
(62) Sun, B. Y.; Inoue, T.; Shimade, T.; Okazaki, T.; Sugai, T.; Suenaga, K.; Shinohara, H. *J. Phys. Chem. B* **2004**, *108*, 9011−9015.
(63) Kodama, T.; Ozawa, N.; Miyake, Y.; Sakaguchi, K.; Nishikawa, H.; Ikemoto, I.; Kikuchi, K.; Achiba, Y. *J. Am. Chem. Soc.* **2002**, *124*, 1452−1455.
(64) Dunsch, L.; Kuran, P.; Kirbach, U.; Scheller, D. *Fullerenes: Recent Advances in the Chemistry and Physics of Fullerenes and Related Materials*; The Electrochemical Society, Inc.: Pennington, NJ, 1997; Vol. 4, pp 523−536.
(65) Xu, J. X.; Lu, X.; Zhou, X. H.; He, X. R.; Shi, Z. J.; Gu, Z. N. *Chem. Mater.* **2004**, *16*, 2959−2964.